

## Spin saturation of the random antiferromagnet (Cd,Mn)Te in magnetic fields to 150 T

E. D. Isaacs

*AT&T Bell Laboratories, 600 Mountain Avenue, Murray Hill, New Jersey 07974*

D. Heiman, X. Wang, and P. Becla

*Francis Bitter National Magnetic Laboratory, Massachusetts Institute of Technology, Cambridge, Massachusetts 02139*

K. Nakao,\* S. Takeyama, and N. Miura

*Institute for Solid State Physics, University of Tokyo, Roppongi, Minato-ku, Tokyo 106, Japan*

(Received 14 March 1990; revised manuscript received 22 October 1990)

Spin alignment of magnetic  $\text{Mn}^{2+}$  ions in the random antiferromagnet  $\text{Cd}_{1-x}\text{Mn}_x\text{Te}$  is studied in high magnetic fields. Faraday-rotation measurements at  $T \sim 10$  K were made up to 150 T for magnetic concentrations ranging from  $x = 0.1$  to 0.6. For  $x = 0.1$  and 0.2 the applied fields are large enough to overcome the internal antiferromagnetic exchange fields, leading to total spin saturation,  $\langle S_z \rangle = \frac{5}{2}$ , at  $B = 80$  and 130 T, respectively. For higher concentrations the spin alignment becomes increasingly difficult due to the increasing number of neighboring spins. A mean-field model that takes into account the random site occupation self-consistently fits the measured field and concentration dependencies of  $\langle S_z \rangle$  remarkably well.

### I. INTRODUCTION

The magnetic alloy  $\text{Cd}_{1-x}\text{Mn}_x\text{Te}$  is an ideal material for studying the properties of a dilute, frustrated antiferromagnet.<sup>1-3</sup> This class of materials exhibits a broad range of magnetic behavior: (i) a paramagnetic-like phase for low concentrations ( $x < 0.05$ ); (ii) a spin-glass-like phase at moderate concentrations; and (iii) a short-range antiferromagnetic phase for high concentrations ( $x \sim 1$ ). The magnetic ions sit on an fcc sublattice. In the limit  $x = 1$  they exhibit type-III magnetic ordering at low temperature,<sup>4</sup> where a given spin has eight nearest neighbors (NN) antiparallel and four parallel, while all six next-nearest neighbors (NNN) are antiparallel. While simple models have been successful in describing the low- and high-concentration regions, the additional complexity of the random distribution in the intermediate regime has impeded the development of a useful model. In the present study we examine the magnetic-field-induced spin alignment of  $\text{Mn}^{2+}$  ions for a range of concentrations from  $x = 0.1$  to 0.6 in magnetic fields to 150 T. These results are of particular interest for modeling bound magnetic polarons, where internal magnetic fields can be as high as 250 T.<sup>5</sup>

In the limit  $x = 1$  the average spin alignment  $\langle S_z \rangle$  of  $\text{Cd}_{1-x}\text{Mn}_x\text{Te}$  in an applied magnetic field  $B$  is expected to be that of a conventional three-dimensional antiferromagnet. In this case,  $\langle S_z \rangle$  increases monotonically for increasing  $B$  and saturates abruptly at  $\langle S_z \rangle = \frac{5}{2}$  at very high magnetic fields ( $B \gg 100$  T). At the other extreme,  $x \ll 1$ , the spin alignment is well described by a Brillouin function appropriate to a modified paramagnet.<sup>6</sup> The term "modified" implies that the magnetic ions are not well isolated from one another and many ions have close neighbors. These neighbors are typically antiferromagnetically coupled and produce an exchange field that op-

poses the applied field. Thus, for increasing  $x$  the exchange field becomes larger requiring a larger applied field to reach spin saturation. In the region  $x < 0.05$ ,  $\langle S_z \rangle$  is described quantitatively by taking into account small clusters of magnetic ions: *singlets*, having no NN; *pairs*, having only one NN per ion; and *triplet* clusters.<sup>7-11</sup> Above  $x = 0.05$  larger clusters must be included, however, they are difficult to model. Evidence of these larger clusters is seen empirically in measurements to 45 T, where a component of  $\langle S_z \rangle$  that is linear in field and whose magnitude increases with  $x$  is observed (see Ref. 10). This linear component has been identified with the response of larger clusters and the infinite network of NN spins.

In this study we describe the spin alignment of  $\text{Cd}_{1-x}\text{Mn}_x\text{Te}$  for the concentrations  $x = 0.1$  to 0.6 in magnetic fields to 150 T. Faraday-rotation measurements were made in a single-turn, exploding coil magnet. The sample temperature before the high-field pulse ( $\sim 6$   $\mu\text{sec}$  pulse duration) was in the range  $T_S = 6-10$  K. The  $B$  field and  $x$  dependencies of  $\langle S_z \rangle$  were fit to model calculations. This model includes the exact response of clusters with three ions or less, as well as the response of larger clusters using a self-consistent mean-field model that accounts for the random site occupation of an ion's nearest neighbors.

### II. EXPERIMENTAL TECHNIQUES

$\text{Cd}_{1-x}\text{Mn}_x\text{Te}$  boules were grown by the Bridgman method with nominal  $x$  values of 0.1, 0.2, 0.3, 0.4, 0.5, and 0.6. Experiments were performed on polished platelets whose thicknesses were chosen to give at least a few full rotations of the transmitted beam by 100 T. For example, the  $\text{Cd}_{0.8}\text{Mn}_{0.2}\text{Te}$  gave slightly more than  $2.5 \times 180^\circ$  of rotation by 100 T for a thickness of 0.46 mm

(see Fig. 1). A He-Ne laser provided linearly polarized light at a wavelength of  $1.15 \mu\text{m}$ . The beam was transmitted through the sample normal to the face of the platelet and along the field direction (Faraday configuration). A polarization beam splitter was placed in the transmitted beam to select the two orthogonal components of the rotated beam. These two beams were focused into separate fiber optic cables leading to photodiodes. These signals were monitored during the magnet shot by transient digitizers.<sup>11</sup>

Both Faraday-rotation and magnetic-field profiles during the  $6\text{-}\mu\text{sec}$  field pulse were collected for each sample. Figure 1 shows an example of the Faraday signal as a function of time for  $x=0.2$  at  $T_S=8\text{ K}$ . Each oscillation corresponds to  $180^\circ$  of rotation of the incident light. The Faraday data were subsequently converted to rotation angle versus magnetic field  $B$  (see Fig. 2). Absolute values for  $\langle S_z \rangle$  as a function of  $B$  were derived from measurements of  $\langle S_z \rangle$  in a dc magnetic field of  $B=5\text{ T}$ . The errors in the high-field values for  $\langle S_z \rangle$  were estimated at  $\pm 10\%$ .

The samples were mounted in a helium-flow cryostat made of thin phenolic resin and kapton pipes. The initial temperature  $T_S$  was monitored with a thermocouple sensor placed very close to the sample. Just prior to a field pulse the temperature was typically  $6\text{--}8\text{ K}$ . During the field pulse the sample temperature could not be accurately monitored.

We have, however, determined an upper limit for the rise in temperature of the crystal by assuming that all of the work done by the magnetic field on the magnetic ions goes into heating the lattice. The magnetic work is given by  $Q = \int H dM$ , where  $M = (2\mu_B x A) \langle S_z \rangle$  in  $\text{J/mol K}$ ,  $A$

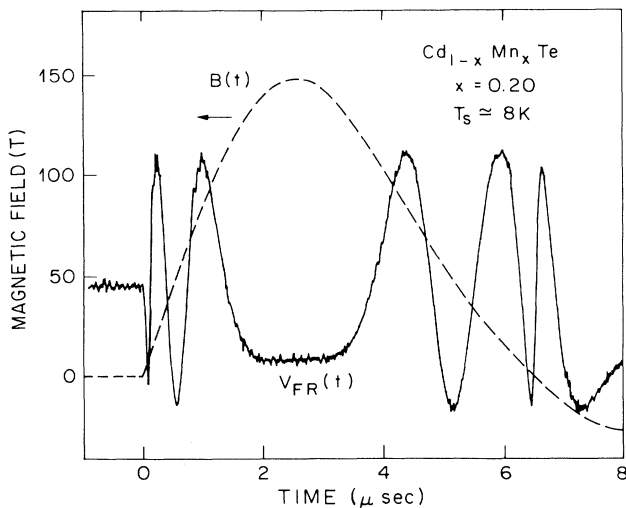


FIG. 1. Faraday-rotation signal for  $\text{Cd}_{1-x}\text{Mn}_x\text{Te}$ ,  $x=0.2$ , vs time for a pulsed magnet shot. The solid line represents the intensity of light that passes a linear polarizer placed at  $45^\circ$  to the incident light polarization at  $B=0\text{ T}$ . The sample temperature at the beginning of the magnet shot is  $T_S \approx 8\text{ K}$ . The magnetic-field trace vs time is shown by the dashed line, where the peak of the field  $B(t)$  is  $150\text{ T}$ .

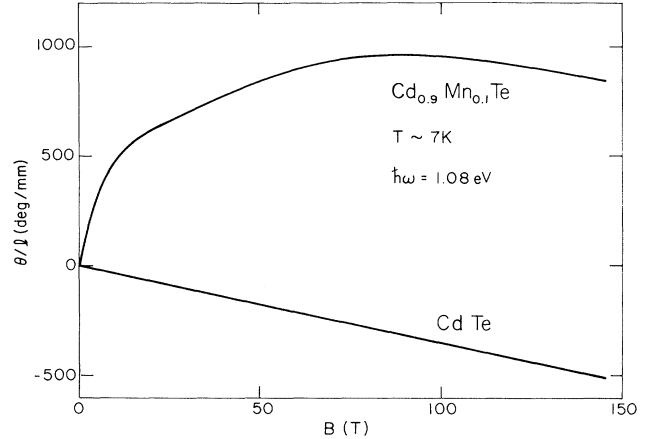


FIG. 2. Faraday-rotation angle per unit thickness of sample,  $\theta(B)/l$ , vs magnetic field  $B$  for  $\text{Cd}_{1-x}\text{Mn}_x\text{Te}$ ,  $x=0$  and  $0.1$ . The sample temperature at the start of the pulse was  $T \approx 7\text{ K}$  and the energy of the incident photon beam was  $1.08\text{ eV}$ .

is Avogadro's number and  $\mu_B = 9.26 \times 10^{-24}\text{ J/T}$ . For  $x=0.1$  (see Fig. 2) the integral was numerically evaluated and gave  $Q \approx 80\text{ J/mol}$ . For  $\text{Cd}_{0.9}\text{Mn}_{0.1}\text{Te}$ , the specific heat varies from  $C \sim 2\text{ J/mol K}$  at  $T=10\text{ K}$  to  $C \sim 16\text{ J/mol K}$  at  $T=20\text{ K}$  ( $C \sim T^3$ ),<sup>11</sup> so that the temperature of the sample is warmed by less than  $10\text{ K}$  during the pulse. For this amount of heating we expect little change in the high field  $\langle S_z \rangle$ . This simple calculation assumes that the spins are paramagnetic and that the spins are always in thermal equilibrium with the lattice during the  $6\text{-}\mu\text{sec}$  field pulse. The first assumption is certainly not true and the effect of interacting spins reduces the net amount of work done by the field. Less work means a smaller temperature rise. Measurements of the spin-lattice relaxation time (see Ref. 13) of less than a few microseconds for  $x \geq 0.1$  at  $T \geq 10\text{ K}$  makes the second assumption reasonable.

Pulsed magnetic fields up to  $150\text{ T}$  with a duration of  $6\text{ }\mu\text{sec}$  were generated by discharge of a  $100\text{-kJ}$ ,  $40\text{-kV}$  fast condenser bank across a single-turn coil with a bore diameter of  $1\text{ cm}$ .<sup>14</sup> A typical field pulse is shown by the dashed line in Fig. 1. Each high-field pulse vaporized the copper magnet coil, but the cryostat and sample remained intact since the coil exploded outward. The field was monitored through the time integration of a pickup coil located inside the cryostat near the sample.

### III. FARADAY ROTATION

Faraday rotation is a simple and powerful technique with which to measure magnetic properties, such as magnetization, of diluted magnetic semiconductors in pulsed magnetic fields (for example, see Ref. 9). Other, more direct techniques, such as magnetization measurements relying on the flux induced in electrical coils, are more difficult due to the large induced emf from the field pulse.<sup>15</sup>

The Faraday angle  $\theta$ , or angle of rotation of plane polarized light propagating along the  $B$ -field direction, is

traditionally expressed as

$$\theta = \frac{\omega d}{2c} (n_- - n_+), \quad (1)$$

where  $\omega$  is the frequency of the incident photon,  $d$  is the path length through the sample,  $c$  is the speed of light in vacuum and  $n_-$  and  $n_+$  are the refractive indices for left- and right-hand circularly polarized light, respectively. A difference in the refractive index for the different polarizations results from the Zeeman splitting of the conduction and valence bands and the optical selection rules that couple them. In wide gap diluted magnetic semiconductors the large  $sp-d$  exchange interaction leads to unusually large Zeeman splitting which gives rise to the so-called giant Faraday rotation.<sup>16</sup>

For the cubic zinc-blende structure of  $\text{Cd}_{1-x}\text{Mn}_x\text{Te}$   $\theta$  can be shown to be of the form

$$\theta = \left[ \frac{2Ed}{3\hbar nc} \right] x \langle S_z \rangle (\alpha N_0 - \beta N_0 / 6) \sum_i g_i f_i E_p^2 \frac{E_{i0}}{(E_{i0}^2 - E^2)^2}. \quad (2)$$

Here,  $\alpha N_0 = 0.22$  eV and  $\beta N_0 = -0.88$  eV are the exchange energies for the conduction and valence band for  $\text{Cd}_{1-x}\text{Mn}_x\text{Te}$ ,<sup>17</sup>  $x$  is the manganese concentration, and  $E = \hbar\omega$ . The sum over the band states corresponds to the real part of the dielectric function where  $E_{i0}$  is the zero-field band gap,  $f_i$  the oscillator strength,  $g_i$  the density of oscillator states, and the plasma energy is given by  $E_p = 4\pi\hbar^2 Ne^2/m$ .<sup>18</sup> Equation (2) is appropriate when  $E$  is far from resonance with the band edge oscillators. When  $E$  is close to resonance the excitonic states must also be included in the sum.

#### IV. EXPERIMENTAL RESULTS

The Faraday-rotation angle per unit thickness of sample,  $\theta(B)/l$ , for  $\text{Cd}_{0.9}\text{Mn}_{0.1}\text{Te}$  is shown in Fig. 2. The contribution to the Faraday rotation not associated with the manganese ions, measured in pure CdTe, is also shown in Fig. 2. This contribution is shown to be linear in field and opposite in sign to the magnetic ion contribution. After subtracting the negative background from the Faraday data for each of the six different concentrations the results could then be scaled to dc measurements at  $B = 5$  T to give  $\langle S_z \rangle$  [see Eq. (2)]. The results are shown by the solid lines in Fig. 3 for  $x = 0.1, 0.2, 0.3,$  and  $0.5$  at  $T \sim 10$  K. These data were taken on the upward side of the magnetic-field pulse. The data on the downward side of the pulse were nearly identical. For  $x = 0.1$  and  $0.2$  the applied field is large enough to overcome the NN exchange fields, and total saturation,  $\langle S_z \rangle = \frac{5}{2}$ , is observed at  $B = 80$  T and  $B = 130$  T, respectively. For increasing  $x$  there is a substantial decrease in the average spin alignment. This is due to the increasing number of NN spins and thus the increasing internal exchange field that a given spin must overcome. For  $x = 0.5$  the spin alignment is almost perfectly linear in field up to 140 T.

In general,  $\langle S_z \rangle$  can be described as arising from three components: (a) small clusters of spins whose total spin aligns relatively easily with the applied field; (b) at

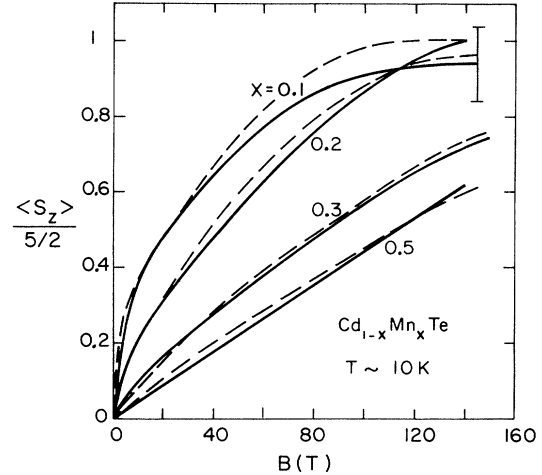


FIG. 3. Average spin alignment  $\langle S_z \rangle$  vs magnetic field  $B$  for  $\text{Cd}_{1-x}\text{Mn}_x\text{Te}$ . Experimental results, shown by the solid curves, were obtained from Faraday-rotation experiments in a single-turn pulsed magnet of 6- $\mu\text{sec}$  duration. Calibration of the Faraday rotation to  $\langle S_z \rangle$  was made by dc magnetization measurements at  $B = 5$  T, resulting in a 10% uncertainty in  $\langle S_z \rangle$  at high fields. Sample temperatures were approximately  $T \cong 10$  K at the start of the magnet pulse. The dashed curves represent model calculations that include small clusters of magnetic ions exactly, and large clusters using a self-consistent mean-field model that incorporates the random site occupation of an ion's nearest neighbors.

moderate fields the total spin of these clusters increases; and (c) an infinite network of antiferromagnetically coupled spins that behave like a defected three-dimensional antiferromagnet, i.e., exhibit a linear field dependence until saturation is reached. For example, for  $x = 0.1$  we observe an "elbow" at about 10 T, which is evidence of the saturating alignment of the small clusters. The linear component above  $B = 10$  T that saturates by 80 T is composed of both (b) and (c). In contrast, for  $x = 0.5$  we only observe a linear field dependence to  $\langle S_z \rangle$ , which is mainly due to (c). These behaviors are described in detail in the following section.

#### V. THEORY

The spin alignment  $\langle S_z \rangle$  can be modeled by considering two contributions: (i) small clusters of nearest-neighbor ions consisting of single ions, pairs, and triplets; and (ii) a paramagnetic mean-field contribution that accounts for the various local environments of a given spin by including random site occupation, self-consistently. Only NN interactions are included explicitly since the NN exchange energy  $J_{\text{NN}}$  is five times larger than further-neighbor interactions.<sup>19,20</sup>

The first contribution, (i), includes only clusters of three spins or less. These clusters dominate  $\langle S_z \rangle$  at low  $x$  and become increasingly less important with increasing  $x$ . The total  $\langle S_z \rangle$  is computed from the sum of individual cluster contributions  $\langle S_z \rangle_i$ , and weighted by the probabilities  $P_i$  of finding an ion in a cluster of type  $i$ , assum-

ing that the  $\text{Mn}^{2+}$  ions are located randomly in the lattice.<sup>1,7,8</sup> In the following,  $B_S(y)$  is the Brillouin function for a spin cluster with quantum number  $S$ ,  $y = gS\mu_B B/k_B T$  and

$$f_S(y) = \frac{\sinh \left[ \left( 1 + \frac{1}{2S} \right) y \right]}{\sinh \left[ \frac{y}{2S} \right]} . \quad (3)$$

For singlets  $S = \frac{5}{2}$ ,

$$P_S = (1-x)^{12} , \quad (4)$$

and

$$\langle S_z \rangle_S = SP_S B_S(y) . \quad (5)$$

For a pair of ions on NN lattice sites, having spins  $\mathbf{S}_1$  and

$\mathbf{S}_2$  then  $\mathbf{S} = \mathbf{S}_1 + \mathbf{S}_2$ ,

$$P_p = 6x(1-x)^{18} , \quad (6)$$

and

$$\langle S_z \rangle_p = P_p \frac{\sum_{S=0}^5 SB_S(y) f_S(y) \exp[JS(S+1)/k_B T]}{\sum_{S=0}^5 f_S(y) \exp[JS(S+1)/k_B T]} . \quad (7)$$

For closed triplets (three ions with each ion having the other ions as NN) with spins  $\mathbf{S}_1$ ,  $\mathbf{S}_2$ , and  $\mathbf{S}_3$ , then there are two spin quantum numbers for the cluster,  $\mathbf{S}_a = \mathbf{S}_1 + \mathbf{S}_2$ , and  $\mathbf{S}_b = \mathbf{S}_1 + \mathbf{S}_2 + \mathbf{S}_3$ ,

$$P_{CT} = 8x^2(1-x)^{23} , \quad (8)$$

and

$$\langle S_z \rangle_{CT} = P_{CT} \frac{\sum_{S_a=0}^5 \sum_{S=|S_a-5/2|}^{|S_a+5/2|} SB_S(y) f_S(y) \exp[JS(S+1)/k_B T]}{\sum_{S_a=0}^5 \sum_{S=|S_a-5/2|}^{|S_a+5/2|} f_S(y) \exp[JS(S+1)/k_B T]} . \quad (9)$$

For open triplets (three ions with the two outer ions  $\mathbf{S}_1$  and  $\mathbf{S}_3$  not as NN), then the two spin quantum numbers are  $\mathbf{S}_a = \mathbf{S}_1 + \mathbf{S}_3$ , and  $\mathbf{S}_b = \mathbf{S}_1 + \mathbf{S}_2 + \mathbf{S}_3$ ,

$$P_{OT} = 6x^2(1-x)^{23} [5(1-x) + 2] , \quad (10)$$

and

$$\langle S_z \rangle_{OT} = P_{OT} \frac{\sum_{S_a=0}^5 \sum_{S=|S_a-5/2|}^{|S_a+5/2|} SB_S(y) f_S(y) \exp\{J[S(S+1) - S_a(S_a+1)]/k_B T\}}{\sum_{S_a=0}^5 \sum_{S=|S_a-5/2|}^{|S_a+5/2|} f_S(y) \exp\{J[S(S+1) - S_a(S_a+1)]/k_B T\}} . \quad (11)$$

Next, we consider the contributions to  $\langle S_z \rangle$  from all other magnetic ions, in clusters of four or more ions, in a self-consistent mean-field model. In this model each ion has, in addition to the applied field, an exchange field due to the surrounding NN ions. We write this as

$$\langle S_z \rangle_{MF} = S \sum_{n=0}^{12} P(n) B_S \left[ (Sg\mu_B/k_B T) \left( B + \frac{2J_{NN}(1-\xi)n \langle S_z \rangle_{MF}}{g\mu_B} \right) \right] , \quad (12)$$

where

$$P(n) = C_{12}^n x^n (1-x)^{12-n} , \quad (13)$$

is the probability that one spin has  $n$  nearest-neighbors on the face-centered cubic cation (Cd) sublattice,  $g=2$ , and  $S = \frac{5}{2}$ . The adjustable parameter  $\xi$  is included to account for neighbors further than NN. We note that  $\xi$  and  $T$  are not independent in Eq. (12) and thus our determination of  $\xi$  is not unique. We have subtracted the effects of singlets, pairs, and triplets when  $n < 4$ , since they have already been included above.

The total  $\langle S_z \rangle$  is then written as

$$\langle S_z \rangle = \langle S_z \rangle_S + \langle S_z \rangle_p + \langle S_z \rangle_{CT} + \langle S_z \rangle_{OT} + \langle S_z \rangle_{MF} . \quad (14)$$

This was fit to the data in Fig. 3 using  $J_{NN}/k_B = 6.1$  K (Ref. 21) and adjusting  $\xi$  for each  $x$  value. Results for the fit are shown in Fig. 3 by the dashed lines. Good overall agreement is found over the entire concentration range from  $x=0.1$  to 0.6. The deviation for  $x=0.1$  at saturation, about 10%, is attributed to the uncertainty in calibrating the experimental curve at low fields.

## VI. CONCLUSIONS

The average spin alignments of the magnetic  $\text{Mn}^{2+}$  ions in the random antiferromagnet  $\text{Cd}_{1-x}\text{Mn}_x\text{Te}$  have been measured up to 150 T for concentrations ranging from  $x=0.1$  to 0.6 at  $T \sim 10$  K. For  $x=0.1$  and 0.2 the applied fields are large enough to overcome the internal

antiferromagnetic exchange fields — total spin saturation,  $\langle S_z \rangle = \frac{5}{2}$ , is observed at  $B=80$  and 130 T, respectively. For higher concentrations the spin alignment becomes increasingly difficult due to the increasing number of neighboring spins. A mean-field model that takes into account the random site occupation of magnetic ions, self-consistently, fits the measured field and concentration dependences of  $\langle S_z \rangle$  remarkably well.

\*Present address: Superconducting Research Laboratory, International Superconductivity Technology Center, Shinonome, Koto-ku, Tokyo 135, Japan.

<sup>1</sup>S. Oseroff and P. H. Keesom, in *Dilute Magnetic Semiconductors*, edited by J. Kossut and J. K. Furdyna (Academic, New York, 1988), Vol. 25, p. 73.

<sup>2</sup>J. K. Furdyna, *J. Appl. Phys.* **61**, 3526 (1987).

<sup>3</sup>Y. Shapira, *J. Appl. Phys.* (to be published).

<sup>4</sup>T. Gieboltowicz, B. Lebech, B. Buras, W. Minor, H. Kepa, and R. R. Galazka, *J. Appl. Phys.* **55**, 2305 (1984); T. Gieboltowicz and T. M. Holden, in *Dilute Magnetic Semiconductors* (Ref. 1), p. 162.

<sup>5</sup>P. A. Wolff, D. Heiman, E. D. Isaacs, P. Becla, S. Foner, L. R. Ram-Mohan, D. H. Ridgely, K. Dwight, and A. Wold, in *High Magnetic Fields in Semiconductor Physics*, edited by G. Landwehr (Springer-Verlag, New York, 1987).

<sup>6</sup>J. A. Gaj, R. R. Planel, and G. Fishman, *Solid State Commun.* **29**, 435 (1978).

<sup>7</sup>S. Nagata, R. R. Galazka, D. Mullin, H. Akbarzadeh, G. D. Khattak, P. H. Keesom, and J. K. Furdyna, *Phys. Rev. B* **22**, 3331 (1980).

<sup>8</sup>Y. Shapira, S. Foner, D. H. Ridgely, K. Dwight, and A. Wold, *Phys. Rev. B* **30**, 4021 (1984).

<sup>9</sup>A. Twardowski, H. J. M. Swagten, W. J. M. de Jonge, and M. Demianiuk, *Phys. Rev. B* **36**, 7013 (1987).

<sup>10</sup>D. Heiman, E. D. Isaacs, P. Becla, and S. Foner, *Phys. Rev. B* **35**, 3307 (1987).

<sup>11</sup>R. R. Galazka, S. Nagata, and P. H. Keesom, *Phys. Rev. B* **22**, 3344 (1980).

<sup>12</sup>N. Miura, T. Goto, K. Nakao, S. Takeyama, and S. Sakakibara, in *Megagauss Technology and Pulsed Power Applications*, edited by C. M. Fowler, R. S. Caird, and D. J. Erickson (Plenum, New York, 1987), p. 209.

<sup>13</sup>D. Scalbert, J. Cernogora, A. Mauger, and C. Benoit à la Guillaume, *Solid State Commun.* **69**, 453 (1989).

<sup>14</sup>K. Nakao, F. Herlach, T. Goto, S. Takeyama, T. Sakakibara, and N. Miura, *J. Phys. E* **18**, 1018 (1985).

<sup>15</sup>S. Takeyama, K. Amaya, T. Nakagawa, M. Ishizuka, K. Nakao, T. Sakakibara, T. Goto, N. Miura, Y. Ajiro, and H. Kikuchi, *J. Phys. E* **21**, 1025 (1988).

<sup>16</sup>J. A. Gaj, R. R. Galazka, and M. Nawrocki, *Solid State Commun.* **25**, 193 (1978).

<sup>17</sup>J. A. Gaj, in *Diluted Magnetic Semiconductors*, Vol. 25 of *Semimetals and Semiconductors* (Academic, New York, 1988).

<sup>18</sup>L. M. Roth, *Phys. Rev.* **133**, A542 (1964); and references cited therein.

<sup>19</sup>D. U. Bartholemew, J. K. Furdyna, and A. K. Ramdas, *Phys. Rev. B* **34**, 6943 (1986).

<sup>20</sup>X. Wang, D. Heiman, P. Becla, and S. Foner, *Phys. Rev. B* **41**, 1135 (1990).

<sup>21</sup>E. D. Isaacs, D. Heiman, P. Becla, Y. Shapira, R. Kershaw, K. Dwight, and A. Wold, *Phys. Rev. B* **38**, 8412 (1988).